OBSERVATION OF THE MAGNETIC DOMAIN IN THIN-FILM HEADS BY ELECTRON MICROSCOPY

Kazuo Kobayashi

Fujitsu Laboratories Ltd., 10-1 Morinosato-Wakamiya, Atsugi 243-01, Japan

Abstract---Magnetic domains were observed using an image lock-in technique for backscattered electron contrast (Type II) with a 200 kV scanning electron microscope. Backscattered electrons indicate a difference in magnetic domain structures at the upper and lower parts of the upper pole in thin-film heads, changing the acceleration voltage. With this method, it is also possible to observe the domain structure of the thin-film head pole through a 10 to 20 μm protective layer, and the upper shield of the MR head through the coil in the resist, alumina overcoat, and upper pole.

I. INTRODUCTION

It is extremely important to observe the domain structure of thin-film magnetic heads to understand the head characteristics. In particular, dynamic magnetization behavior is essential in understanding the various types of noise occurring in the head.

The dynamic magnetization behavior of thin-film heads has been observed using a scanning Kerr effect microscope (SKEM) [1-4], which only detects surface information of the metal magnetic materials and does not give sufficient resolution. Therefore we used a scanning electron microscope to observe the magnetic domain of thin-film heads.

II. EXPERIMENT

Using a JEOL 2000FXII 200 kV scanning electron microscope, we observed the magnetic domain with an image lock-in technique originated by Wells [5] and developed by Ferrier [6], for backscattered electron contrast (Type II), as shown in Figure 1 [7-9]. A special double gap objective lens polepiece (BMP20) shielded the specimen from the magnetic field. A 10 mAp-p, 100 kHz drive current excited the thin-film head. A serial pair of diode detectors and lock-in amplifier synchronously detected backscattered electrons (BSEs). To obtain the wall contrast of the magnetic domain, we positioned a pair of detectors symmetrically to the electron beam axis above the specimen, and the incident electron beam was normal to the specimen surface [10]. We used LINK eXL-II system to acquire digital images. We usually acquired 16 bit 256x256 pixel images with a dwell time of 5 ms, giving 5 minutes per frame.

We tested heads with and without protective layers. We plated NiFe poles on the heads. The 3-μm thick 83.5 wt.% Ni poles had 8-μm wide cores. We also used plating to fabricate a two-layer 32-turn coil.

We also tested the MR head. The 3.5 μm thick upper shield and upper pole were both made by NiFe plating. The widths of the upper shield and the upper pole were about 200 μm, and 6 μm, respectively.

III. LOCK-IN PRINCIPLE

Figure 2 shows an example of domain contrast without a lock-in amplifier for the 10-μm thick NiFe thin-film. The dark and bright contrast of the walls depends on the direction of magnetization of the domains.

The lock-in amplifier has a low-pass filter and a PSD (phase-sensitive detector) and multiplies input signals,

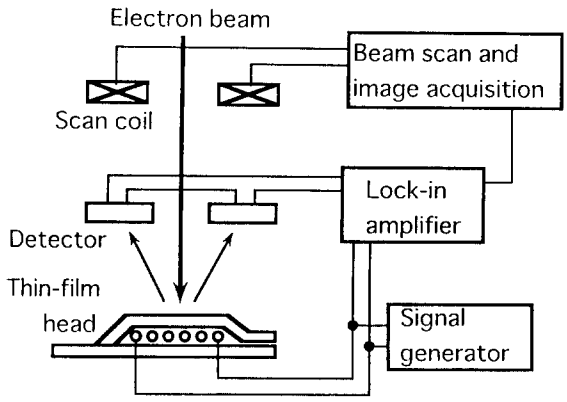

Fig. 1 Experimental setup.

including noise and reference signals. The output from a lock-in amplifier is proportional to the amplitude of the signal component synchronized with a reference signal. Figure 3 shows the waveforms of a lock-in processed image for the case where the domain contrast caused a sinusoidal displacement of the domain wall [5]. Here, an electron beam stops at one position, and the wall, which displaces sinusoidally (maximum amplitude S_m), meets the electron beam on the line AA'. The distance between the meeting point and the displacement center of the wall is S.

The waveform F(t) that is obtained with the BSE detector is shown in Figure 3(b). The output is zero except for brief pulses at instants when the electron beam meets the wall. If the time for this is λT, where T is the period of the sinusoidal displacement of the wall, then λ is given by

$$\cos 2\pi\lambda = S_r = S/S_m$$

Since the lock-in amplifier only detects the amplitude of the signal component synchronized with the reference signal, the lock-in amplifier output is given by the $\cos\omega t$ coefficient A_1 of the Fourier series F(t). Since F(t) is an even function, A_1 is given by

$$A_1 = \frac{2}{T}\int_{-\frac{T}{2}}^{\frac{T}{2}} F(t)\cos\omega t\, dt = \frac{4}{T} S_r$$

The detected signal is shown in Figure 3(c). The domain wall is detected as a pair of black and white lines, whose location indicates the maximum limit of domain wall movement in a synchronous mode [9, 10].

Fig. 2 Wall contrast of 10 μm NiFe thin-film.

IV. RESULTS AND DISCUSSION

A. Images of Thin-Film Head without Protective Layer

Figure 4 shows an example of images of the thin-film head's magnetic domain structure without a protective layer. The accelerating voltage of the electron beam is around 80 kV here. It shows a clear closure domain structure. A pair of black and white lines shows which domain wall exists. Figure 4(a) is the magnetic domain in the upper pole, (b) is the pole tip region, (c) shows the assumed directions of magnetization vectors in the head. Figure 4(d) shows the BSE image when signals bypass the lock-in amplifier.

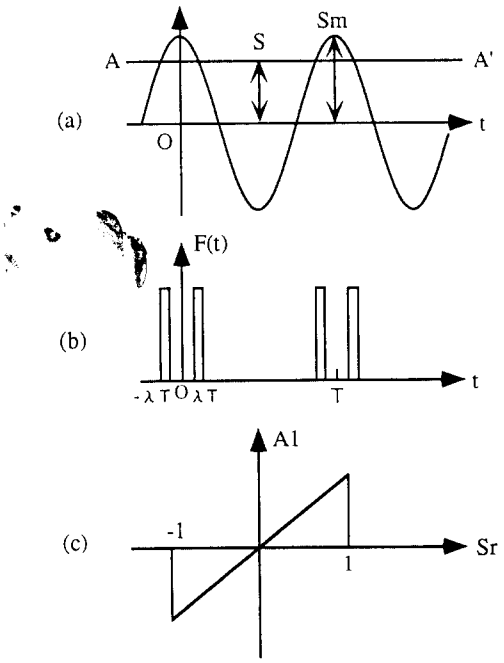

Fig. 3 Waveforms in lock-in processed image for domain contrast.

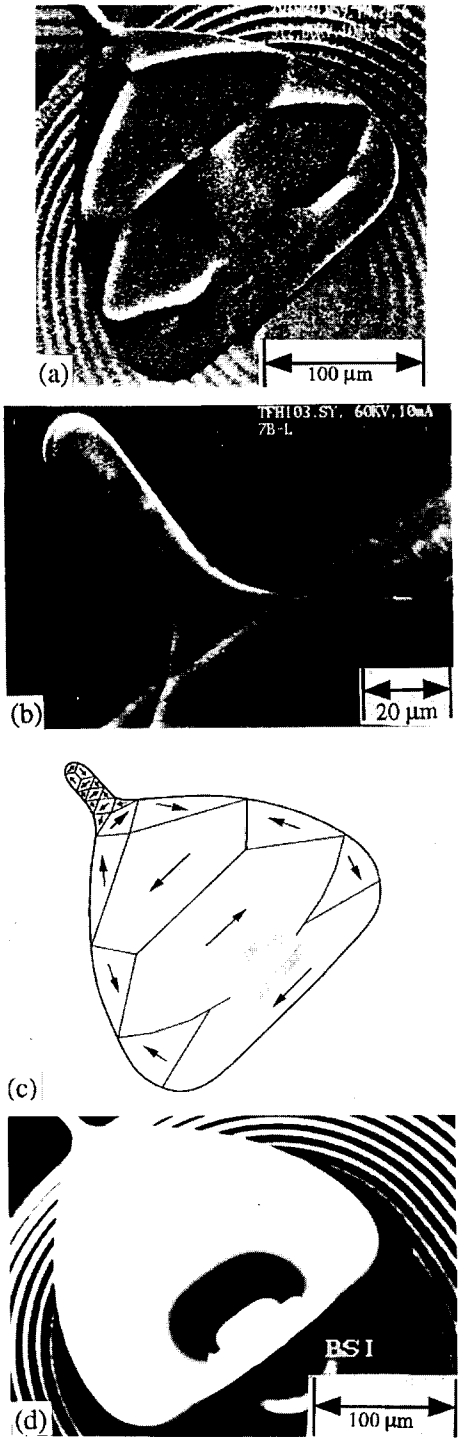

Fig. 4 Images of thin-film head: (a) magnetic domain in the upper pole, (b) magnetic domain in the pole tip, (c) supposed domain structure, (d) backscattered electron image.

B. Dependence on Drive Current

The results obtained at various head currents using the same head as in Figure 4 were shown in Figure 5. As the head current was increased, the interval between the black and white lines increased, which indicates the maximum limit of domain wall movement in synchronous mode.

The positions of white and black lines are reversed at A and B in Figure 5(c), indicating that the phases of wall motion are shifted 180° . This means that the domains on the right and left each have magnetization components which are opposite to the direction of flux in the head tip, as shown schematically in Figure 4(c).

C. Dependence on Accelerating Voltage

Figure 6 shows the closure domain structure at various accelerating voltages. The accelerating voltage was gradually raised (Figures 6(a) to (d)). Although there is no change in the domains near the tip of the pole, the domain walls near the backgap (indicated by the arrows in Figure 6(a)) gradually

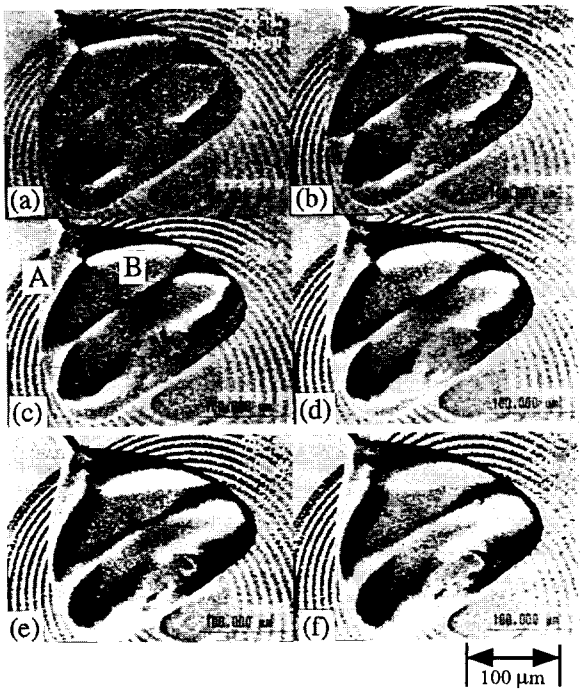

Fig. 5 Changes in the synchronously detected images for different drive currents: (a) 5 mA, (b) 10 mA, (c) 20 mA, (d) 30 mA, (e) 40 mA, (f) 50 mA.

change. When the accelerating voltage is raised, the BSEs emitted from the sample are known to originate from deeper parts. According to Tsuno, BSEs can detect information from depths of 0.2, 1, and 6 μm, using acceleration voltages of 50, 100, and 200 kV [10]. Therefore the 60 kV image in Figure 6(a) corresponds to the upper layer of the pole, and in Figure 6(d) at 160 kV, the lower layer of the pole.

The domain structures near the backgap are different, as shown in Figures 5(a) and (d). This difference indicates that the positions of wall motion are different in the upper and lower layers of the pole, since we can synchronously detect only the moving parts of the walls by the lock-in technology.

Mallary has proposed a model where the flux flow at high frequencies is due to both domain wall movement and magnetization rotation [11]. Hence the differences in domain wall motion observed here represent different manners of flux flow. The walls marked by the arrows in Figure 6(d) move on the outer sides of the pole unlike in Figure 6(a), which means the flux entering or leaving from the backgap is spread throughout the head in the lower layer of the pole. Therefore the flux tends to concentrate more in this head on the axis of symmetry of the headpole. Moreover wall motion is particularly vigorous in the lower left of the figure.

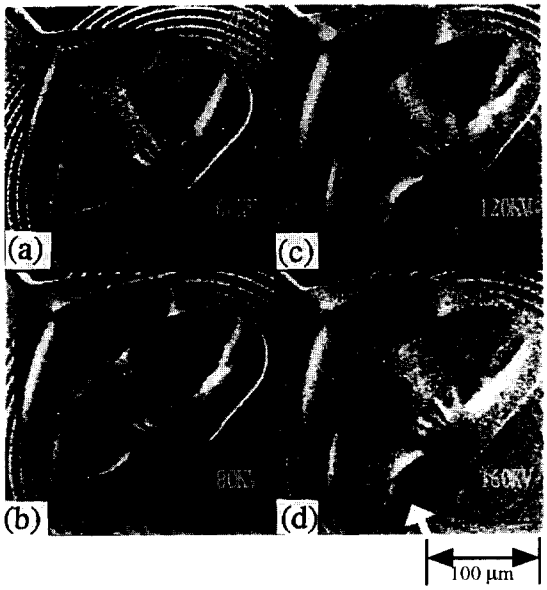

Fig. 6 Changes in the synchronously detected images for different accelerating voltages: (a) 60 kV, (b) 80 kV, (c) 120 kV, (d) 160 kV.

D. Images of Thin-Film Head with Protective Layer

We observed the thin-film head with a protective layer, since it is possible to observe the magnetic domain structure of the head pole through a 10 to 20 μm thick protective layer using the lock-in technique. Figure 7 shows the magnetic domains of heads with different compositions to the NiFe

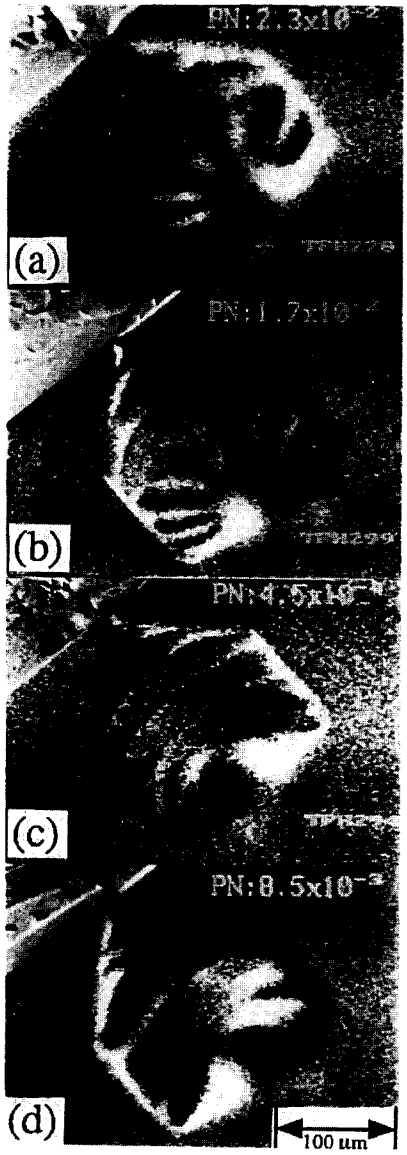

Fig. 7 Magnetic domains of heads with different compositions of NiFe pole: (a and b) 83.5 wt.% Ni, (c and d) 82.5 wt.% Ni.

Journal of Korean Magnetics Society, Volume 5, Number 5, October 1995

pole. The accelerating voltage and current applied to the head were chosen here to be 200 kV and 20 mAp-p respectively.

Heads with 83.5 wt.% Ni composition exhibit radial domain walls (domains with circular arc-like magnetization) centered at the backgap closure, as shown in Figures 7(a) and (b). These radial walls originate from the negative magnetostriction of the head pole and the circumferential tensile stress centered at the backgap closure [12].

Heads with 82.5 wt.% Ni composition with zero magnetostriction exhibit closure domain structure (Figures 7(c) and (d)). The walls near the backgap closure are rather circumferential around it, which means the magnetic pole has a small amount of positive magnetostriction.

E. Images of Upper Shield of MR Head

We also observed the upper shield of the MR head. The MR head was composed of a lower shield, lower gap alumina, an MR element, upper gap alumina, an upper shield, a coil in the resist, an upper pole, and an alumina protective layer, from the bottom of the substrate. The lower pole and upper shield were merged in this head. We observed the upper shield of MR head with 200 kV accelerating voltage, 120 mAp-p drive current. The alumina overcoat was polished to get a better resolution to the point just before the upper pole appeared. The dwell time for image data acquisition was set at 40 ms here.

Figure 8 shows the domain structure of the MR head. The domain structure of the upper shield was shown in Figure 8(a), and its schematic domain structure was also shown in Figure 8(c). We observed a good closure domain structure was through the coil in the resist, alumina overcoat, and upper pole.

Figure 8(b) shows the domain structure of the upper pole of the MR head for comparison, observed at 100 kV accelerating voltage, with 120 mAp-p drive current. The walls moved sharply because of the high drive current for the upper pole. The domain structure of the upper pole was not observed clearly (Figure 8(a)), because it was observed at 200 kV accelerating voltage when the electron beam penetrates the upper pole.

V. CONCLUSION

Using a scanning electron microscope, we observed the magnetic domain structure in a thin-film head and a MR head with an image lock-in technique for backscattered electron contrast. Backscattered electrons indicate a difference in the magnetic domain structure at the upper and lower parts of the upper pole, changing the acceleration voltage, which is not

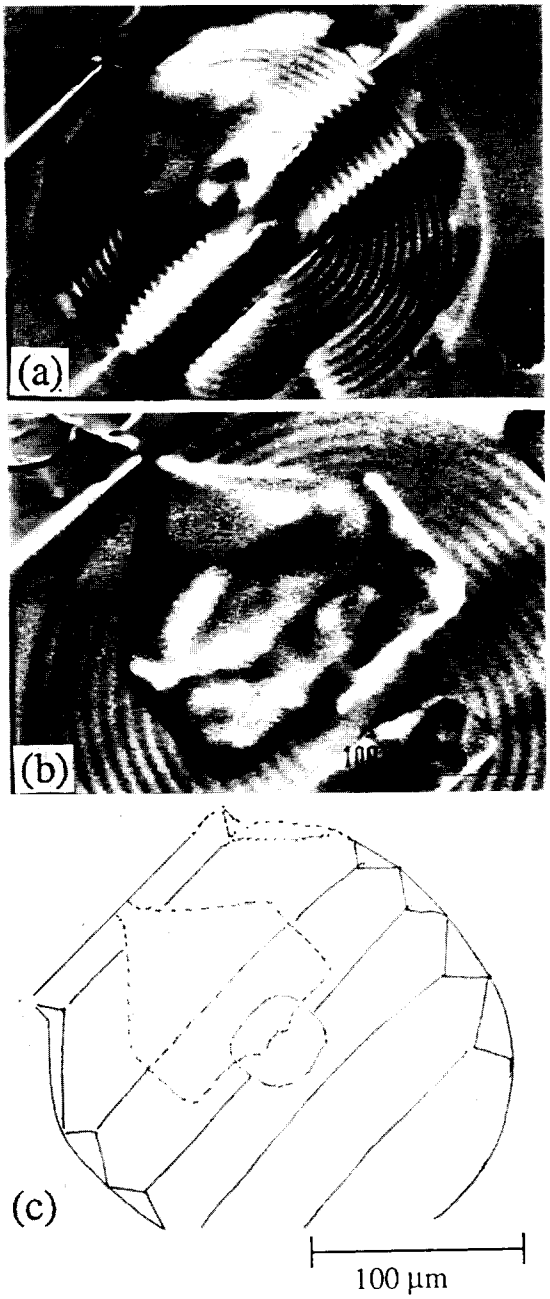

Fig. 8 Magnetic domains of MR head: (a) upper shield (200 kV), (b) upper pole (100 kV), (c) supposed domain structure of upper shield.

possible by an optical method such as SKEM. This method can also be used to observe the domain structure of a thin-film head pole through a 10 to 20 μm protective layer, and the upper shield of an MR head through the coil in the resist, alumina overcoat, and upper pole.

ACKNOWLEDGMENTS

We thank Professor R. P. Ferrier of the University of Glasgow for his assistance and instruction in the lock-in technique. We also thank Mr. M. Otagiri for his assistance.

REFERENCES

[1] P Kasiraj, R. M Shelby, J. S Best, and D. E. Horne, *IEEE Trans. Magn.*, vol. **MAG-22**, 837 (1986).

[2] P. L. Trouilloud, B. E. Argyle, B. Petek, and D. A. Herman, *IEEE Trans. Magn.*, vol. **MAG-25**, 3461 (1989).

[3] B. Petek, P. L. Trouilloud, and B. E. Argyle, *IEEE Trans. Magn.*, vol. **MAG-26**, 1328 (1990).

[4] S. Narumi, S. Sudo, M. Aihara, and H. Fukui, *J. Magn. Soc. Jpn.*, vol. **16**, 95 (1992). (Japanese)

[5] O. C. Wells and R. J. Savoy, *IEEE Trans. Magn.*, vol. **MAG-17**, 1253 (1981).

[6] R. P. Ferrier, S. McVitie, and W. A. P. Nicholson, *IEEE Trans. Magn.*, vol. **MAG-26**, 1337 (1990).

[7] K. Kobayashi, *J. Mag. Soc. Jpn.*, vol. **17**, 117 (1993). (Japanese)

[8] K. Kobayashi, *J. Mag. Soc. Jpn.*, vol. **18**, 103 (1994). (Japanese)

[9] K. Kobayashi, *IEEE Trans. Magn.*, vol. **MAG-30**, 3933 (1994).

[10] K. Tsuno, *Rev. Sol. State Science*, vol. **2**, 623 (1988).

[11] M. Mallary, A. Torabi, and M. H. Kryder, *J. Appl. Phys.*, vol. **67**, 4863 (1990).

[12] H. Koyanagi, R. Arai, K. Mitsuoka, H. Fukui, S. Narishige, and Y. Sugita, *J. Mag. Soc. Jpn.*, vol. **13**, 103 (1989). (Japanese)